Published in Journal of Vacuum Science & Technology A 9, issue 3, 1663-1669, 1991
which should be used for any reference to this work

Boron *K*-shell spectroscopy of boron-doped silicon

F. J. Esposto, P. Aebi, T. Tyliszczak, and A. P. Hitchcock
Institute for Materials Research and OCMR, McMaster University, Hamilton L8S 4M1, Canada
M. Kasrai and J. D. Bozek
Department of Chemistry and OCMR, University of Western Ontario, London, Ontario N6A 5B7, Canada
T. E. Jackman and S. R. Rolfe
Institute for Microstructural Sciences, National Research Council, Ottawa K1A 0R6, Canada

The B *K*-edge spectra of various model compounds (BF_3, KBF_4, B_2O_3, $B(OH)_3$, orthocarborane ($B_{10}H_{10}C_2H_2$) and elemental boron) were investigated to characterize the sensitivity of B *K*-edge spectra to local chemical environment. Electron yield detection of synchrotron photoabsorption at the boron *K*-edge was used to study the B sites in Si(B) epilayers grown by molecular beam epitaxy and *in situ* B doped from evaporated B_2O_3. Although there were interesting spectral variations with composition and annealing, comparison between the x-ray electron yield results and those from secondary ion mass spectroscopy and electrochemical capacitance voltage measurements indicate that the yield spectra are strongly influenced by surface segregation.

I. INTRODUCTION

Recently, many new device structures have been proposed, which are based on the premise that molecular beam epitaxy (MBE) can precisely control the uniformity and distribution of dopants over exceedingly small dimensions.[1,2] However, for the case of silicon MBE,[3] problems such as surface segregation, low incorporation probabilities, and clustering of the dopants has hindered progress.[4] In principle, boron (incorporated by coevaporation using sources ranging from elemental boron,[5] to boron-doped silicon[6] to HBO_2[7,8] to B_2O_4,[9-12] would seem an obvious choice as the p-type dopant because of its lower ionization energy and higher solid solubility. However, recent studies suggest significant redistribution problems.[1-13]

Models of the chemical reactions occurring during boron doping of MBE layers with B_2O_3 have been proposed.[9,12] Essentially, the B_2O_3 is absorbed on the surface and then reacts with incoming Si to decompose to B and Si_xO_y complexes. Further interaction with Si produces SiO which desorbs above a certain temperature. Incomplete reduction of SiO_2 to SiO at lower growth temperatures can lead to oxygen incorporation into the growing lattice. The thermodynamics of oxygen incorporation has been worked out in detail by Tuppen *et al.*[13] and was shown to correspond well with experimental findings.

Secondary ion mass spectrometry (SIMS) and electrochemical capacitance-voltage profiling (eCV) have been used by Jackman *et al.*[13,14] to study the effect of substrate temperature on the boron incorporated by coevaporation of B_2O_3. This study clearly demonstrated significant redistribution and clustering of boron at growth temperatures above 700 °C.[14] As the substrate temperature was lowered, it was found that one could obtain abrupt interfaces and layers with electrical activity far in excess of the solubility limit of boron in Si, but that there was significant oxygen incorporation (as high as 1.5 times the amount of boron). The temperature dependence of the oxygen-to-boron ratio in both highly and lightly doped samples agrees fairly well with the thermodynamic model of Tuppen *et al.*,[13] although this model does not comment on any interaction between the oxygen and the substitutional boron. In addition, post-growth diffusion of the multilayers showed a strong dependence on the original growth temperature.

Obviously the chemical state and possible role of the oxygen in the electrical activity and boron diffusion are important questions to address. Techniques such as Fourier transform infrared spectroscopy[15] and Raman scattering[16,17] have not shown any evidence for B–O–Si complexes but it is difficult to ascertain whether the negative results are related to the absence of such complexes or simply insufficient sensitivity. X-ray absorption near edge spectroscopy can provide detailed information on local geometric and electronic structure about selected atoms. The sensitivity of X-ray absorption to local structure is particularly valuable for probing the character of point defects, about which most other techniques can provide relatively little structural information. Core excitation spectroscopy is a spatially localized probe of unoccupied density of states in the region of the core excited atom.

For specific reasons related to the preferred bonding modes of boron, B *K*-shell (1*s*) spectra could be an effective tool for differentiating among local environments of boron relevant to boron doping in semiconductors. In many compounds, such as BF_3, BN, B_2O_3 and $B(OH)_3$, where boron is bonded to three atoms in a planar trigonal configuration, the ligand field splits the B 2*p* orbitals resulting in a compact, low-energy, empty B $2p_z$ orbital (*z* is perpendicular to the plane defined by the nearest neighbor atoms). In consequence there is a sharp, intense, low energy electric dipole B $1s \rightarrow$ B $2p_z$ excitation in these species. On the other hand, there are other boron environments, such as the icosahedra of elemental boron,[18] the polyhedra of borane and carborane complexes,[19] or the tetrahedral substitutional site of boron in a Si lattice, in which each boron atom is coordinated by four

or more other atoms. In these structures rehydridization spreads the empty B $2p_z$ density over a wider range of energies so that the B K spectra of boron in these environments might not be expected to exhibit the sharp, low energy spike characteristic of trigonal environments. The possibility that the presence or absence of a low energy B $1s \rightarrow$ B $2p_z$ could be used to distinguish trigonal and nontrigonal environments has been discussed previously by Hallmeier *et al.*,[20] who performed electron yield measurements of B K spectra of a range of boron-containing minerals. Blau *et al.*[21] have further elaborated this concept. They propose that boron in high symmetry environments (spherical, tetrahedral, or octahedral) should exhibit only a single broad band (since the B $2p$ orbitals remain triply degenerate in these symmetries) while boron in lower symmetry environments (cylindrical, hexagonal, tetragonal or trigonal) would exhibit at least two bands with the lower energy one being rather sharp (in the symmetry groups mentioned the B $2p$ orbitals would split into a "π" and a "σ" component). Very recently McLean *et al.*[22] have reported the B K-edge spectrum of the Si(111)–B($\sqrt{3}$x$\sqrt{3}$)R 30° surface state in which boron is approximately tetrahedrally coordinated.[23] This spectrum exhibits a broad s-polarized band at 191 eV and a strong, p polarized, low energy peak at 188.6(5) eV. The latter feature is unexpected for tetrahedrally coordinated boron according to the concepts proposed by Hallmeier *et al.*[20] and Blau *et al.*[21] We have performed model compound studies in order to further clarify the relationship between B K-edge spectra and local boron coordination.

II. EXPERIMENTAL X-RAY ABSORPTION MEASUREMENTS

The B K-edge spectra were acquired with electron yield detection at the Canadian grasshopper beam line[24,25] of the Synchrotron Radiation Centre (SRC) in Stoughton, Wisconsin. The pressure of the system was 3×10^{-8} Torr and the samples were at ambient temperature (300 K) during measurements. The sample mounting was such that the E vector of the radiation was always in the surface plane and thus polarization studies could not be made. This was not a major limitation for the model compound aspects of this study since they were randomly oriented polycrystalline materials. Electron yield detection[26] is well suited for *hard x-ray* studies of dopants in semiconductors[26-28] since the depth sensitivity is well matched to typical dopant distributions and thicknesses of MBE grown layers. However the technique is less well suited for B K-edge spectroscopy due to the very shallow depth sensitivity in the *soft x-ray* range. Fluorescence detection may have been preferable for this study since it is a deeper probe, but this requires a thin window x-ray detector which was not available for these measurements.

Two techniques were used to measure the electron yield. The first involved using a channeltron to detect electrons ejected from the sample as an amplified current. The second involved measuring the current at the sample. Sample current detection was used for most measurements since the statistical precision was somewhat better. The two techniques measure complementary aspects of the same physical process and thus should provide equivalent information although the acceptance angle of the channeltron is smaller than the 2π sr effective "acceptance angle" of sample current detection.

The incident photon flux (I_0) from the CSRF grasshopper beam line was measured simultaneously as the current at a Au mesh located just upstream of the sample. However, this signal was not useable for most of the spectra since it contained artifacts at the B K-edge region, perhaps due to boron contamination on the gold mesh. It is critical that the I_0 signal does not contain structure in the spectral region of interest, particularly when attempting to study dilute systems. A common alternative I_0 monitor is measurement of the electron yield signal from a substrate free of the element of interest. We attempted to use the photoionization sample current of a Si wafer which had no boron doping, as an accurate measure of the combination of the incident flux and the underlying Si L_{23} extended x-ray absorption fine structure (EXAFS) signal. In many ways this is preferable to a simple I_0 monitor[29] since it corrects for the Si L_{23} EXAFS as well as for variations in the incident photon flux. The single crystal silicon is highly ordered and there is relatively strong Si L_{23} EXAFS. In practice substrate-I normalization did not work satisfactorily. We have found that the best procedure to analyze our measured spectra has been to use the sample current (I) signal without explicit correction for I_0. The reason for the failure of the clean substrate normalization procedure is not fully understood. It may indicate that the time delay between measuring Si(B) and clean Si samples exceeded the time scale of changes in shape of the incident flux spectrum.

III. MODEL COMPOUND STUDIES

The studies by Hallmeier *et al.*[20] of oxide minerals containing BO_3 and BO_4 units show that the B K-edge spectrum of trigonal planar coordinated boron is characterized by a sharp B $1s \rightarrow$ B $2p_z$ transition around 195 eV and suggest that this feature is absent in structures in which boron is not trigonal-planar coordinated. This concept is well illustrated by the boron fluorides. Figure 1 compares the B K-edge spectra of BF_3 (gas) and KBF_4 (solid) along with spectra simulated from extended Hückel MO calculations.[30] The B K-edge spectrum of BF_3 was recorded at McMaster by inelastic electron scattering.[31] It is identical to published x-ray absorption spectra of BF_3.[32,33] The B K-edge spectrum of KBF_4 was digitized from the x-ray electron yield spectrum of the solid.[20] The experimental spectra are shown after background subtraction and have been normalized at 218 eV, in the far continuum. The sharp, intense spike observed in the calculated and experimental spectra of BF_3 is due to the B $1s \rightarrow 2p_z(\pi^*, a_1)$ transition. In contrast, the B K-edge spectrum of KBF_4 does not exhibit a low energy peak. Instead it is dominated by a broad t_2, σ^*(B–F) band at higher energy (200.5 eV). The absence of the low-energy spike in BF_4^- can be rationalized in terms of the sp^2 to sp^3 rehybridization of the boron atom which shifts the empty B $2p_z$ density to higher energy.

The broad feature in the ionization continuum of both BF_3 (205 eV) and KBF_4 (200.5 eV) is attributed to B $1s \rightarrow \sigma^*$(B–F) transitions. The shift to lower energy of the B

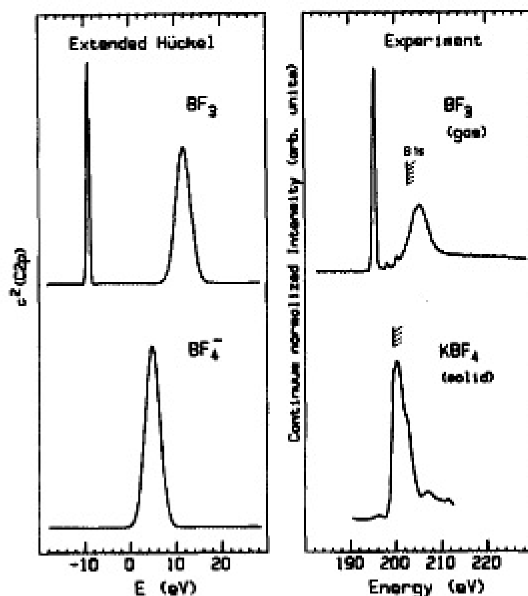

FIG. 1. Comparison of experimental and calculated B K-edge spectra of BF_3 (gas) and KBF_4 (solid). The simulated spectra are derived from eigenvalues and eigenfunctions calculated by extended Hückel theory (EHT) using the equivalent ionic core virtual orbital method (Ref. 30). The inner shell electron loss spectrum of BF_3 was obtained using 2.5 keV impact energy and 2° scattering angle. The spectrum of KBF_4 was measured with synchrotron radiation using electron yield detection (Ref. 20). The experimental spectra have had a smooth background subtracted and have been normalized to the same intensity at 218 eV in the continuum where the cross section is expected to be atomic-like. Both the EHT-simulated and experimental BF_3 and KBF_4 spectra are plotted on common intensity scales. The B 1s ionization potentials are 202.8 eV (BF_3) and 199.8 eV (KBF_4) (Ref. 20).

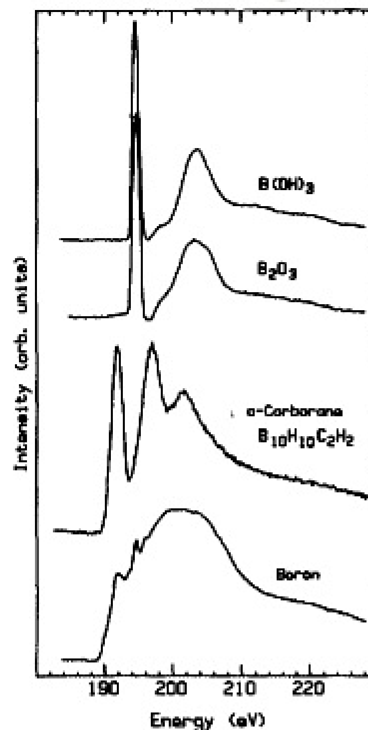

FIG. 2. B K-edge spectra of $B(OH)_3$, B_2O_3, and β-rhombohedral boron (s) measured by synchrotron photoabsorption with electron yield detection and o-carborane (g) measured by electron impact.

$1s \rightarrow \sigma^*$(B–F) transition in KBF_4 relative to that in BF_3 is consistent with the longer B–F bond length in BF_4^- (1.38 Å) than in BF_3 (1.31 Å), according to the documented correlation of $1s \rightarrow \sigma^*$ energies and bond lengths.[34] The weak features observed between the π^* and σ^* features in BF_3 are Rydberg states.[20,32,33] The fine structure superimposed on the main peak in the KBF_4 spectrum may be related to multiple scattering from more distant coordination shells.

Figure 2 plots the boron K-edge spectra on an absolute energy scale of $B(OH_3)$, B_2O_3, o-carborane[35] and elemental boron. The x-ray electron yield spectra of $B(OH)_3$ and B_2O_3 are somewhat better resolved but otherwise in good agreement with those reported by Hallmeier *et al.*[20] As expected from their very similar BO_3 trigonal local environment,[18] the spectrum of B_2O_3 is very similar to that of $B(OH)_3$. The spectrum of each exhibits a sharp spike at 195 eV, corresponding to the B $1s \rightarrow 2p_z(\pi^*)$ transition, and a broad feature at 202 eV, corresponding to B $1s \rightarrow \sigma^*$(B–O) transitions. The B K-edge electron yield spectrum of elemental boron shows similar features but with greater contrast than in the true photoabsorption spectrum reported by Kizler *et al.*[36] Consistent with the concept proposed by Hallmeier,[20] the B K-spectrum of elemental boron does *not* exhibit a strong low energy spike but rather consists of a series of broad structures spanning a wide energy range. The weak feature around 195 eV may be associated with surface oxide, since it is not evident in the spectrum of Kizler *et al.*[36] Since the local boron coordination is rather similar to that of elemental boron one might have expected o-carborane ($B_{10}H_{10}C_2H_2$) to have a similar B K-edge spectrum. However, this spectrum, recently recorded in the gas phase by electron impact,[35] contains a sharp low lying feature at 192 eV. The shift of the first feature in the B K-edge spectrum of o-carborane to lower energy relative to that in the trigonal oxides and fluorides is consistent with the lower oxidation state of boron in o-carborane. This trend is continued further in boride compounds,[37] where the lowest energy feature, which is also a relatively sharp, well-isolated peak, occurs at 188 eV, similar to the position of the low energy peak in the B K-edge spectrum of Si(111)–B($\sqrt{3} \times \sqrt{3}$)R 30°.[22]

Thus the model compound studies (Figs. 1 and 2) suggest that the B K-spectra of trigonal planar coordinated boron will be characterized by an intense, sharp peak which should occur around 195 eV for cationic boron. Structures with a different boron coordination are significantly different, in general shifting to lower energy for less oxidized boron, as expected from electrostatic chemical shift concepts. The o-carborane spectrum clearly indicates that the presence of a low-lying peak is not specific to trigonal planar coordinated boron. However, the combination of characteristic spectral shapes and the energy of the lowest excitation does allow considerable insight into the local boron environment. The model compound spectra suggest that, if boron K-shell near

edge spectra can be acquired at the dilute concentrations typical of boron doping, these may be useful in distinguishing electrically active tetrahedral substitutional boron dopant sites from other forms in which boron could be incorporated into diamond–lattice semiconductors.

IV. MOLECULAR BEAM EPITAXY STUDIES

A. Sample preparation

The growth procedures and molecular beam epitaxy facility have been described in detail previously.[14] Briefly, the epilayers were grown on standard, 100-mm-diam Czochralski wafers in a Vacuum Generators V80 Silicon MBE facility. The boron doping was carried out by co-evaporation of B_2O_3 from a shuttered evaporation cell. SIMS spectra were recorded with a Cameca IMS 4*f* ion microprobe and the secondary ion yields were calibrated using ion-implanted reference standards. Carrier concentrations were measured with a Polaron PN4200 eCV profiler. Post-growth annealing was carried out on some pieces in a standard UHV furnace to remove oxygen from the epilayers. The sample characteristics are summarized in Table I. Because of the extreme surface sensitivity of the electron yield detection techniques, the native oxide layer was removed by etching with concentrated HF acid, rinsed in deionized water, and dried with N_2 gas immediately prior to insertion into the measurement chamber via a load lock.

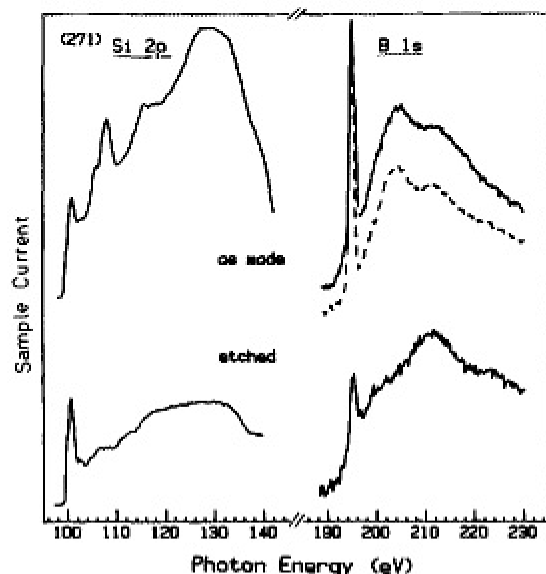

FIG. 3. Comparison of the Si L_{23} $(2p)$ and B K spectra from the high concentration as-grown sample (no. 271, with 3×10^{20} at. cm^{-3} of boron in the outer 0.1 μm according to SIMS) before and after etching. The background subtracted spectra have not been corrected for the incident flux (see the text for rationalization). The sharp drop after 130 eV is related to second order C 1s signal in the transmission function of the monochromator. The dashed line is a simulation of the B K-edge spectrum of the nonetched sample as a weighted sum of the spectrum of the etched sample (40%) and that of B_2O_3 (60%).

B. Effect of etching of Si L_{23} and B K-edge spectra: Depth sensitivity of electron yield detection

Background subtracted Si L_{23} $(2p)$ and B K-edge electron yield spectra of the as-prepared high-boron sample (no. 271) are shown in Fig. 3. The spectra recorded before and after HF etching show significant changes in both the Si L and B K regions. Essentially the same results with regard to the effect of etching were found for all of the Si(B) samples studied.

The observation of both Si and SiO_2 related signals at 100 and 108 eV, respectively, in the Si L_{23} spectra of the unetched sample allows an estimation of the depth sensitivity of sample current (electron yield) detection at the B K edge. Since the ratio of the intensities of features associated with bulk Si (100 eV) and SiO_2 (108 eV) is approximately 1:1, the depth sensitivity must be of the order of 40 Å, assuming the standard protective oxide of $\sim$20 Å thickness. Silicon–oxide growth measurements performed by M. Monita *et al.*[38] indicated that less than 5 Å of oxide should regrow during the time between HF dip etching and pumpdown.

The B K-edge spectrum of the as-made material is reminiscent of that of $B(OH)_3$ and B_2O_3 (Fig. 2) although the broad continuum structure is more complex and the sharp peak at 195 eV is less intense. After etching, the intensity of the 195 eV "oxide" spike in the B K-spectrum is greatly reduced and the broad maximum at 205 eV disappears. The changes in the boron spectra with etching can be explained as follows. In the nonetched sample, the detected signal is produced by boron primarily in the surface silicon oxide layer. Thus the boron atoms are in an oxygen-rich environment and are likely to have a local structure similar to that in B_2O_3 or $B(OH)_3$. It is assumed that etching removes the boron oxide along with the surface silicon oxide layer, hopefully revealing a spectrum representative of the chemical environment of boron in the bulk of the silicon epilayer. The spectrum after etching (Fig. 3) retains a 195 eV spike, although it is much weaker than that in the oxide surface layer. The fact that the peak does not shift to lower energy indicates that the boron contributing to the spectrum after etching is still in the form of some type of BO_x complex, but it is probably not completely oxidized (i.e., $1<x<3$). If the boron atoms were in a tetrahedral substitutional environment then there should be structure below 190 eV.[12]

The change in the oxide character with etching can be understood in terms of removal of B_2O_3-like material since a 6:4 linear combination of the boron spectrum of B_2O_3 with that of etched sample no. 271 gives an excellent match to the B K-edge spectrum of the as-grown, nonetched material (see dashed line in Fig. 3). The estimated B_2O_3/BO_x ratio is similar to the relative contributions of the silicon oxide and bulk silicon signals in the Si L_{23} spectrum suggesting that one chemical form of the near-surface boron is selectively removed by etching.

C. Effect of annealing of the B K-edge spectra of the surface boron environment

Figure 4 shows the B K-edge spectra of the as-grown and annealed samples for two of the materials studied. In each

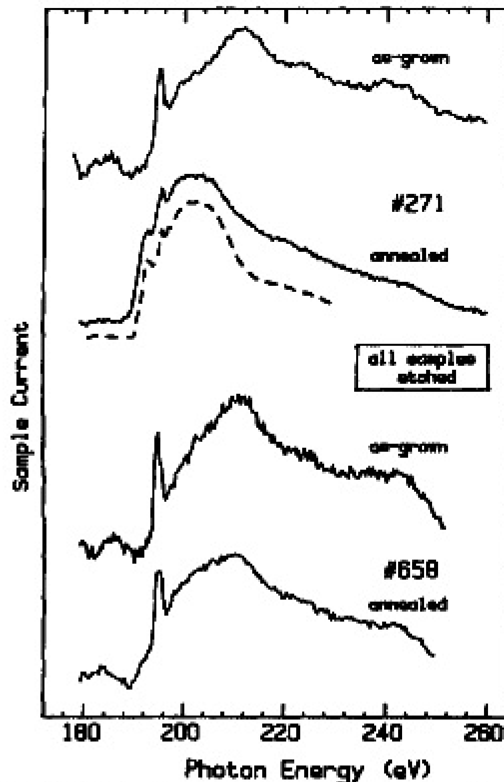

FIG. 4. Comparison of the B K-edge spectra of the high (no. 271) and low (no. 658) concentration samples, as-grown and after vacuum annealing at 900 °C for 2 h. The spectra were measured by sample current detection on Si(B) samples etched just prior to study. A smooth background extrapolated from the preedge region has been subtracted in each case. The feature around 184 eV is a Si L_{23} EXAFS oscillation. The dashed line just below the spectrum of annealed no. 271 is the spectrum of elemental boron.

case the samples were etched to remove the surface oxide layer immediately before installation in the vacuum chamber. Surface segregation of boron appears to strongly affect these results. The intensity of the B 1s ionization continuum (at 215 eV) relative to that at the Si L-edge spike at 100 eV (which is characteristic of bulk silicon) has been used to estimate the *amount* of boron that is contributing to the detected x-ray signal. These results are summarized in Table I for all four samples. If the boron in the surface layer sampled by the current detection scheme is in fact representative of the bulk boron, then one would expect the boron signal in no. 658 to be four times smaller than that in no. 271 for the as-made samples. This is not the case. The absolute boron concentration can also be estimated. The B 1s cross section at 215 eV is 1.5 times the Si 2p cross section at 100 eV based on boron and silicon spectra normalized in the continuum to atomic cross sections[39] [see footnote (d) of Table I for further details]. This cross-section ratio has been used to convert the relative B 1s/Si 2p spectral intensities to boron concentrations ($\pm 50\%$) in the layer sampled by the electron yield x-ray measurements. These values (Table I) show that the x-ray spectral data (surface) are *inconsistent* with the SIMS (bulk) both in terms of the absolute and the relative amounts of boron in the no. 271 and no. 658 samples. The amount of boron in the surface region is more than an order of magnitude greater than that in the bulk of the epilayer measured by SIMS. In fact, boron constitutes a large fraction of the surface atoms instead of the actual doping level of less than 1%.

We suggest that the BO_x structure deduced from the B K-edge spectra of the first 40 Å represents a surface residue at the end of the epitaxial growth (or the annealing process) and that it is not relevant to the chemical environment of

TABLE I. Oxygen, boron, and carrier concentrations in as-made and annealed Si(B) determined by SIMS and x-ray electron yield measurements.

	SIMS			XAS		Activity [carrier]	
	[O][a]	[B][b]					
Code	(at. cm^{-3})	(at. cm^{-3})	B(at. %)	Raw[c]	B(at. %)[d]	Pred.[e]	eCV
No. 658							
As-made	1×10^{19}	8×10^{19}	0.16	0.10	7	1×10^{19}	3×10^{19}
Anneal[f]	$<2\times10^{18}$	7×10^{19}	0.14	0.15	10	8×10^{19}	6×10^{19}
No. 271							
As-made	1×10^{20}	3×10^{20}	0.60	0.13	9	1×10^{19}	8×10^{19}
Anneal[f]	2×10^{19}	9×10^{19}	0.18	0.17	11	8×10^{19}	8×10^{19}

[a] Average SIMS concentration in the epilayer determined by 10 keV Cs^+ bombardment with O^- detection. Note, although SIMS indicates a very uniform concentration throughout the full epilayer, determining accurate concentrations in the outer 50 Å by SIMS is very difficult. The estimated accuracy of the bulk epilayer concentration is 10%.

[b] Average SIMS concentration in the epilayer determined by 7.5 keV O_2^+ bombardment with B^+ detection.

[c] Relative boron intensity expressed as ratio of signal above background at 215 eV (B 1s continuum) to that at 100 eV (Si 2p discrete feature). Uncertainties based on replicate determination are 40%.

[d] This estimate of the atomic percent of boron in the region sampled by the x-ray measurements is based on normalization of the B K spectrum of o-carborane and the Si L spectrum of sputtered no. 271 to atomic intensities in the continuum [Si L_{23} (133 eV) to 0.0433 eV^{-1}; B K (220 eV) to 0.0108 eV^{-1} (Ref. 39). The ratio of I(215 eV) is then found to be 1.5 for equivalent amounts of B and Si. Estimated uncertainty is $\pm 50\%$.

[e] Predicted from the solubility limit of boron in Si at the growth or annealing temperature (as measured with B_2O_3 doping (Ref. 41).

[f] Samples annealed in vacuum at 900 °C for 2.5 h. The epitaxial layer in the no. 658 sample was 2.0 μm thick, grown at 700 °C, while that of the no. 271 sample was 0.6 μm thick, grown at 680 °C.

boron in the deeper portions of the silicon epilayer. In order to explore the latter, the as-grown, unetched no. 271 sample was Ar^+ ion sputtered (2 keV, 10 μA) to remove 1000 Å or one-sixth of the doped epilayer as determined by subsequent SIMS measurements. Spectra of this sample before and after sputtering are presented in Fig. 5. We note from the change in the Si *L*-edge shape that the sputtering effectively removes the oxide layer but it also amorphizes the surface region. We did not anneal to remove this damage since we did not wish to cause surface segregation of the boron. Surprisingly, after sputtering B *K*-edge structure could not be detected even after several hours of signal averaging. From the statistical precision of the spectrum of the sputtered sample and simulations of weighted mixtures of a clean, normalized boron spectrum and that of the sputtered no. 271 sample, we estimate the detection limit for boron with our electron yield detection method to be around 0.1 at. %. This is lower than the boron concentration in the no. 271 Si(B) sample (Table I) so we are somewhat surprised that B 1*s* signal was not detected in the sputtered sample. Preferential sputtering of boron is not expected to occur. At present we do not fully understand this result. We note the detection limit deduced by our simulations is similar to that determined from parallel electron energy loss spectra of Si(B) samples recorded in a transmission electron microscope.[40] The principle limitation is overlap with the Si L_{23} extended fine structure.

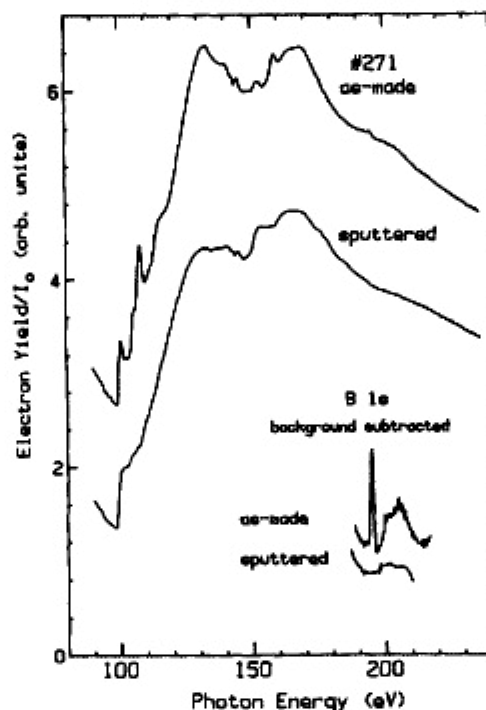

FIG. 5. Comparison of the Si L_{23} and B *K*-edge spectra of (unetched) as-grown sample no. 271 before and after a 10 min Ar^+ ion sputter (10 μA, 2 keV). An identical polynomial background subtraction and intensity scaling has been used in each case to prepare the expansion of the B *K*-edge region. The change in the Si *L*-edge region with sputtering indicates removal of the oxide and amorphization. The dip and structure between 130 and 165 eV arises from Si L_1 (2*s*) ionization and incomplete normalization of second order carbon signal.

It is possible that fluorescence detection, which probes depths of the order of 0.1 μm at the boron edge, may give some advantage for studies of boron doped Si. However the boron *K* fluorescence yield is very small ($<0.01\%$) and it would be extremely difficult to distinguish the weak B *K* (183 eV) emission line from the wings of the much more intense Si *L* line ($\sim$ 80 eV) Because of these factors fluorescence detection of boron in Si is probably not feasible with current x-ray detection technology.

The dramatic change in spectral *shape* with annealing (i.e., the loss of oxygen) of the high boron concentration sample (no. 271) is attributed to a change from a trigonal BO_x environment to one very similar to that of elemental boron. This is deduced from the similarity of the B *K*-edge spectrum of annealed no. 271 to that of elemental boron (see the dashed line in Fig. 4). It is interesting to note that the boron signal from the annealed was significantly stronger than that from the as-grown no. 271 sample, as indicated by the improved statistical precision (Fig. 4). The much improved signal quality is associated with a six fold increase in the detected sample current in both the B *K* and Si *L* regions for essentially the same incident photon flux. Since the boron concentration in the sampled region increased by only 30% according to the ratio of the B *K* and Si L_{23} intensities (see Table I), we suggest the increased signal strength is related to changes in the structure at the surface which decreases the work function and thus increases the depth sampled.

In sharp contrast to the high concentration sample, the shape of the boron spectrum of the lower boron concentration sample (no. 658) does not change appreciably with annealing. This suggests that the boron in the near-surface region of no. 658 is in an environment which is chemically stable at 900 °C. The presence of the 195 eV spike in the spectrum of both the as-made and the annealed no. 658 sample suggests that the near-surface boron remains as a BO_x complex. The absence of changes in the local boron environment with annealing of no. 658 is *not* consistent with the SIMS/eCV results (Table I), which indicate a large *drop* in the oxygen concentration in the first 0.1 μm and some increase in electrical activity. The lack of shape change is consistent with no significant increase in signal strength (i.e., no change in the work function), even though the concentration within the surface region sampled by the current detection technique appears to increase by 50% (Table I). Overall, these results indicate that there are large differences between the chemistry occurring in the outer 30–50 Å and that occurring in the bulk of the 1 μm thick epilayer.

V. SUMMARY

The model compound studies show that B *K*-edge spectroscopy is a sensitive probe of the local structure of boron. The spectrum of boron trigonally coordinated by oxygen consistently exhibits a strong sharp feature around 195 eV but that of boron in other environments can also exhibit low-lying peaks which shift to considerably lower energy for boron in lower oxidation states.

The electron yield spectra of the Si(B) test samples were

found to be dominated by a surface residue rather than the bulk boron environment. However the variations in the Si(B) spectra with etching, annealing and concentration did demonstrate the chemical sensitivity of B *K*-edge spectroscopy. Unfortunately the proximity of the B *K*-edge to the strong Si L_{23} continuum makes it difficult to achieve adequate sensitivity, even at relatively high doping levels.

Finally, this study further reinforces the need to be careful in assuming that the surface region sampled is actually representative of the bulk whenever a highly surface sensitive technique such as soft x-ray photoyield is used. The possibility of large variations in the depth sensitivity of soft x-ray electron yield measurements associated with work function changes should also be noted.

ACKNOWLEDGMENTS

This work has been supported financially by the Natural Science and Engineering Research Council of Canada. S.R.C. is a University of Wisconsin facility funded by NSF. We thank the SRC staff and CSRF beamline personnel, particularly Dr. Kim Tan and Dr. Jin-Ming Chen, for their assistance during our experiments. We also thank R. Brydson, F. Hofer, A. McLean, and F. J. Himsel for useful discussion and comments on drafts of this paper. The samples were supplied by Dr. M. W. Denhoff of the NRC.

[1] G. H. Dohler, CRC Crit. Rev. Solid State Mater. Sci. **13**, 196 (1986).
[2] R. People, IEEE J. Quantum Electron. **22**, 1696 (1986).
[3] J. C. Bean, Science **230**, 127 (1985).
[4] *Silicon Molecular Beam Epitaxy*, edited by K. E. Kasper and J. C. Bean, (Chemical Rubber, Boca Raton, FL, 1988).
[5] R. A. A. Kubiak, W. Y. Leong, and E. H. C. Parker, Appl. Phys. Lett. **44**, 878 (1984).
[6] R. M. Ostrom and F. G. Allen, Appl. Phys. Lett. **48**, 221 (1986).
[7] T. Tatsumi, H. Hirayama, and N. Aizaki, Appl. Phys. Lett. **50**, 1234 (1987); (in press).
[8] T. Tatsumi, H. Hirayama, and N. Aizaki, in *Silicon Molecular Beam Epitaxy II*, edited by J. C. Bean and L. J. Schowalter (Chemical Rubber, Boca Raton, FL, 1988), p. 430.
[9] N. Aizaki and T. Tatsumi, *Extended Abstracts of the 17th Conference on Solid State Devices and Materials* (Japan Society of Applied Physics, Tokyo, 1985), p. 301.
[10] E. de Frésart, S. S. Rhee, and K. L. Wang, Appl. Phys. Lett. **49**, 847 (1986).
[11] J. A. Jackman, P. Williams, T. E. Jackman, and D. C. Houghton, in *Proceedings of the 6th International Conference on Secondary Ion Mass Spectroscopy*, edited by A. Benninghoven and H. W. Werner (Wiley, London, 1988), p. 521.
[12] E. de Frésart, K. L. Wang, and S. S. Rhee, Appl. Phys. Lett. **53**, 48 (1988).
[13] C. G. Tuppens, K. A. Prior, C. J. Gibbons, T. E. Jackman, and D. C. Houghton, Appl. Phys. Lett. **64**, 2751 (1988).
[14] T. E. Jackman, D. C. Houghton, K. Song, J. McCaffrey, M. W. Denhoff, J. A. Jackman and C. G. Tuppen, Appl. Phys. Lett. **53**, 877 (1988).
[15] B. Oliver (unpublished).
[16] A. C. de Wilton, M. Simard-Normandin, and P. T. T. Wong, Can. J. Phys. **65**, 821 (1987).
[17] A. C. de Wilton (unpublished).
[18] E. L. Muetterties, *The Chemistry of Boron and its Compounds* (Wiley, New York, 1967).
[19] K. Wade, *Electron Deficient Compounds* (Nelson, London, UK, 1971).
[20] K. H. Hallmeier, R. Szargan, A. Meisel, E. Hartmann, and E. S. Gluskin, Spectrochimica Acta. A **37** 1049 (1981); W. H. E. Schwarz, L. Mensching, K. H. Hallmeier, and R. Szargan, Chem. Phys. **82**, 57 (1983).
[21] W. Blau, R. Dudde, and H. Petersen, Sol. St. Commun. **69**, 147 (1989).
[22] A. B. McLean, L. J. Terminello, and F. J. Himpsel, Phys. Rev. B **41**, 7694 (1990).
[23] R. L. Headrick, I. K. Robinson, E. Vlieg, and L. C. Feldman, Phys. Rev. Lett. **63**, 1253 (1989).
[24] K. H. Tan, G. M. Bancroft, L. L. Coatsworth, and B. W. Yates, Can. J. Phys. **60**, 131 (1982).
[25] G. M. Bancroft, K. H. Tan, and J. D. Bozek, Phys. Canada **1987**, 113.
[26] T. Tyliszczak and A. P. Hitchcock, Physica B **158**, 335 (1989).
[27] T. Tyliszczak, A. P. Hitchcock, and T. E. Jackson, J. Vac. Sci. Tech. A **8**, 2020 (1990).
[28] A. Erbil, W. Weber, G. S. Cargill III, and R. F. Boehme, Phys. Rev. B **34**, 1392 (1984); K. C. Pandey, A. Erbil, G. S. Cargill III, and R. F. Boehme, Phys. Rev. Lett. **61**, 1282 (1988).
[29] J. Stöhr, *X-ray Absorption, Principles, Applications, and Techniques of EXAFS, SEXAFS and XANES*, edited by D. C. Koningsberger and R. Prins (Wiley, New York, 1988), p. 480.
[30] F. J. Esposto, M. Sc. thesis, McMaster University, 1990.
[31] A. P. Hitchcock, S. Beaulieu, T. Steel, J. Stöhr, and F. Sette, J. Chem. Phys. **80**, 3927 (1984); A. P. Hitchcock, Ultramicroscopy **28**, 165 (1989); Phys. Scr. T **31**, 159 (1990).
[32] V. A. Fomichev, Sov. Phys. Solid State **9**, 2496 (1968); R. L. Barinskii and I. M. Kulikova, Bull. Acad Sci. USSR Phys. Ser. **38**, 16 (1974).
[33] S. V. Nekipelov, V. N. Akimov, and A. S. Vinogradov, Opt. Spectrosc. **64**, 487 (1988); Sov. Phys. Sol. St. **30**, 2095 (1988).
[34] F. Sette, J. Stöhr, and A. P. Hitchcock, J. Chem. Phys. **81**, 4906 (1984).
[35] S. W. Lee, P. A. Dowben and A. P. Hitchcock (to be published).
[36] P. Kizler, E. Hertlein, P. Vargas, and S. Steeb, J. Phys. **47**, C8-1019 (1986).
[37] F. Hofer (unpublished results).
[38] M. Monita, T. Ohmi, E. Hasegawa, M. Kawakami, and K. Suma, Appl. Phys. Lett. **55**, 562 (1989).
[39] B. L. Henke, P. Lee, T. J. Tanaka, R. L. Shimabukuro and B. K. Fujikawa, At. Dat. Nucl. Dat. Tab. **27**, 1 (1982).
[40] R. F. Egerton, Proc. Microsc. Soc. Canada **16** (1990) 20.
[41] G. L. Vick and K. N. Whittle, J. Electrochemical Soc. **116**, 1142 (1969).